Electronic Supplementary Material (ESI) for Analyst.

Supporting Information of

Ultrasensitive detection of dopamine using Au microelectrodes integrated with mesoporous silica thin films

Juan Huang, Huaxu Zhou, Yanqi Zou, Huiqing Liu*, Qianjin Chen*

State Key Laboratory for Science and Technology of Eco-Textile, Ministry of Education, College of Chemistry and Chemical En-gineering, Donghua University, Shanghai, 201620, China

1. SEM images of a bare 25 μm-diameter Au microelectrode

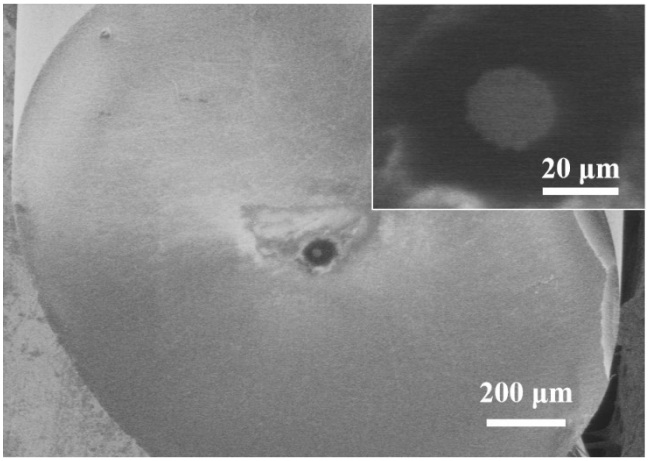

Figure S1. Typical SEM images of the bare 25 μm-diameter Au microelectrode.

2. Optimization of EASA condition

The mesoporous silica thin film was modified on the surface of Au microelectrode by EASA method. We optimized the electrodeposition procedure at Au microelectrodes based on the electrochemical responses of ion ($Ru(NH_3)_6^{3+}$) permeability across the fabricated mesoporous silica thin film and the detailed results are shown as below. Three different potentials (−2.0, −2.2 and −2.5 V) with three different deposition times (2, 5, and 10 s) were investigated and the obtained modified Au microelectrodes were utilized to evaluate the ion permselectivity by voltammetric measurement in 0.5 mM $Ru(NH_3)_6Cl_3$ aqueous solution with 0.1 M KCl. Overall, the modified electrodes prepared at −2.2 V for 5 second exhibited the most significant enhancement of $Ru(NH_3)_6^{3+}$ reduction after surfactant removal (Figure e) with decent ion blockage before surfactant removal (Figure e). These Figures are now included in the Supporting Information.

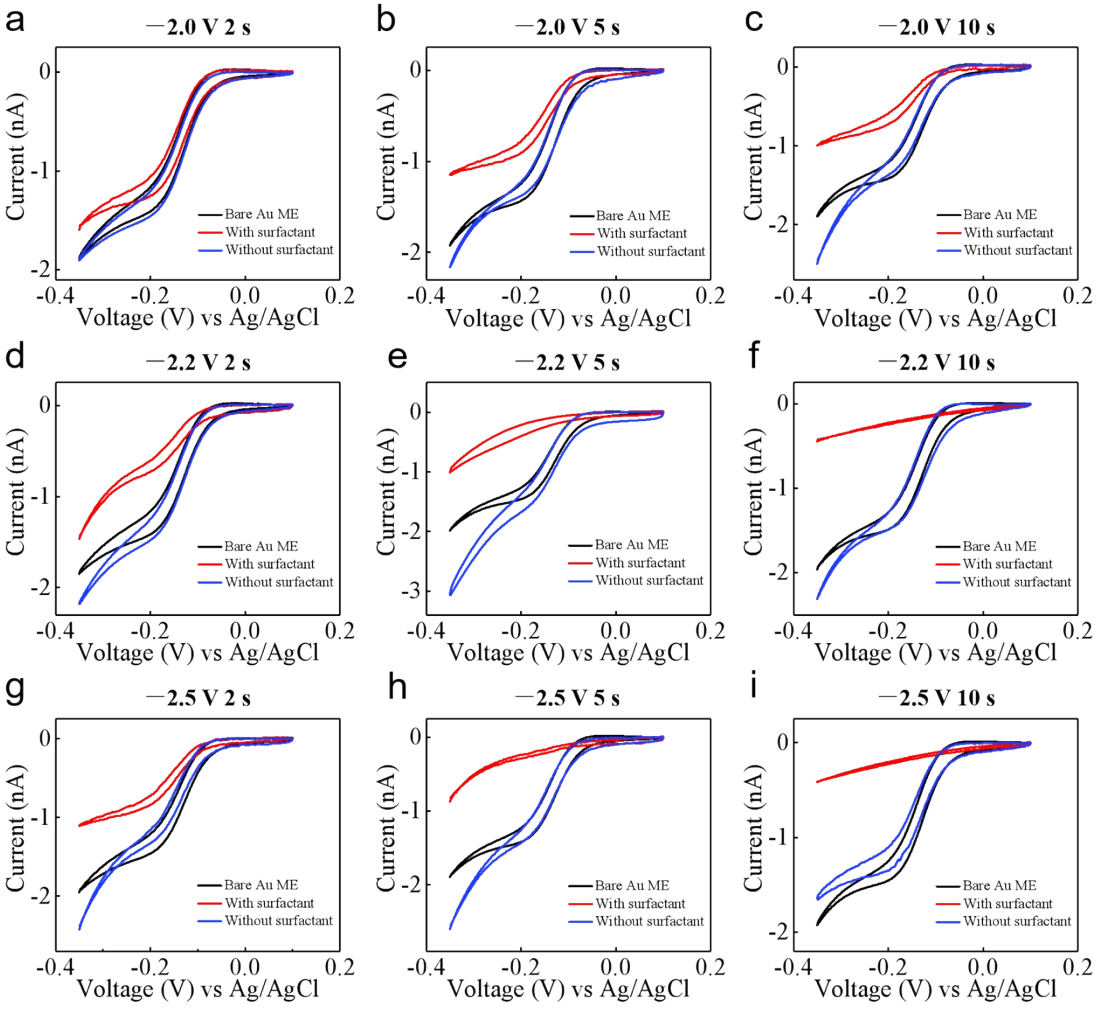

Figure S2. Cyclic voltammetries of 0.5 mM $Ru(NH_3)_6Cl_3$ in 0.1 M KCl aqueous solution at the bare (black curves), and mesoporous silica thin film modified (red curves: before template surfactant removal; blue curves: after template surfactant removal) 25 μm-diameter Au microelectrode in different EASA conditions. Scan rate: 50 mV/s.

3. Optical microscope and SEM images of modified Au microelectrode

In Figure S3 (a) and (c), the bare Au microelectrode shows evident mechanical scratch left from electrode polishing. In Figure S3 (b) and (d), the modified Au microelectrode shows the presence of thin film on the Au surface and the absence of mechanical scratch after electrodeposition.

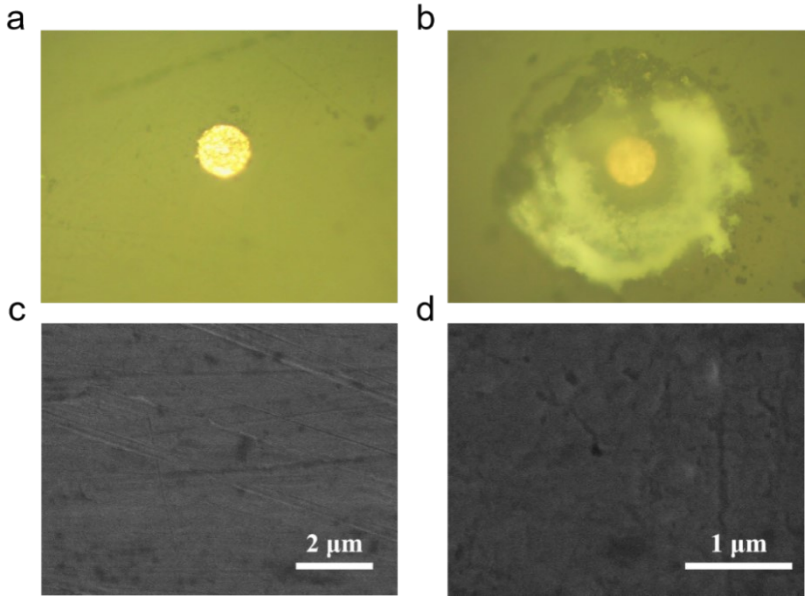

Figure S3. Optical microscope images of (a) bare and (b) mesoporous silica thin film modified 25 µm-diameter Au microelectrode; SEM images of (c) bare and (d) mesoporous silica thin film modified 25 µm-diameter Au microelectrode.

4. The effect of DA accumulation time

Prior to the detection of dopamine, it is crucial to consider its accumulation within the silica films. DPV peak currents were measured across various accumulation times to assess this factor. Equilibrium in the peak current is achieved at 30 seconds indicates that an accumulation time of 30 seconds is optimal for achieving reliable detection results.

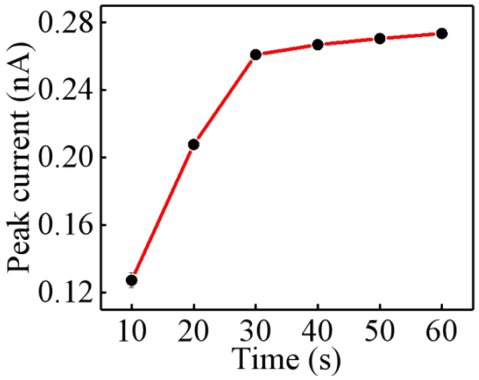

Figure S4. DPV peak currents measured with a mesoporous silica thin film modified 25 μm-diameter Au microelectrode towards DA (10 μM) in 0.1 M PBS buffer (pH = 7.0) at different accumulation time.

5. Comparison of present dopamine sensors with others

Electrode	Method	Linear range (μM)	Detection Limit (μM)	Reference
TMAC–SMCs/ITO	DPV	20 - 226	9.0	[1]
Au/L-Cys/ITO	DPV	2.0 - 400	0.60	[2]
NGr-20/ITO	DPV	4.0 - 40	0.65	[3]
$(PDA\text{-}AuNP)_3$/ITO	DPV	0.20 - 8.0	0.06	[4]
OPEDOT–AuNPs–ERGO/GCE	SWV	4.0 - 100	1.0	[5]
PTGCE	SWV	0.70 - 19.48	0.64	[6]
$NiFe_2O_4$-AC/GCE	DPV	5.0 - 100	0.40	[7]
CoNi-MOF@ERGO/GCE	DPV	0.10 - 400	0.086	[8]
This work	DPV	0.50 - 30	0.084	/

Table S1. Comparison of the performance of past and present dopamine sensors.

ITO: indium tin oxide; TMAC–SMCs/ITO: silica mesochannels and N-Trimethoxy silylpropyl-N,N,N-trimethylammonium chloride modified ITO; Au/L-Cys/ITO: L-Cysteine self-assembled gold nanoparticles modified ITO; NGr-20/ITO: N-graphene films modified ITO; $(PDA\text{-}AuNP)_3$/ITO: Polydopamine and gold nanoparticles modified ITO; GCE: glassy carbon electrode; OPEDOT–AuNPs–ERGO/GCE: overoxidized poly(3,4-ethylenedioxythiophene), gold nanoparticles, and electrochemically reduced graphene oxide modified GCE; PTGCE: poly(2,4,6-trihydroxybenzaldehyde) film modified GCE; $NiFe_2O_4$-AC/GCE: $NiFe_2O_4$ nanoparticles-decorated activated carbon nanocomposite modified GCE; CoNi-MOF@ERGO/GCE: CoNi-MOF and electrochemically reduced graphene oxide modified G.

References

[1] W. Li, L. Ding, Q. Wang and B. Su, *Analyst*, 2014, **139**, 3926–3931.

[2] H. Shen, X. Kong, X. Cao, *Microchem. J.*, 2022, **174**, 107043.

[3] B. Matsoso, B. Mutuma, C. Billing, K. Ranganathan, T. Lerotholi and G. Jones, *Electrochim. Acta.*, 2018, **286**, 29–38.

[4] H. Zhang, F. Zhang, S. Li and H. Li, *Ionics*, 2017, **23**, 2475–2487.

[5] J. Pan, M. Liu, D. Li, H. Zheng and D. Zhang. *J. Pharm. Anal.*, 2021, **11**, 699–708.

[6] S. Elugoke, O. Fayemi, A. Adekunle, F. Adesanya and E. Ebenso, *ChemElectroChem*, 2024, **11**, e202400021.

[7] T. Aparna, R.Sivasubramanian, *J. Chem. Sci.*, 2018, **130**, 14.

[8] Y. Zhou, M. Tian, R. Li, Y. Zhang, G. Zhang, C. Zhang and S. Shuang, *ACS Biomater. Sci. Eng.*, 2023, **9**, 5599–5609.